Cloning, function, and localization of human, canine and *Drosophila* ZIP10 (SLC39A10), a Zn^{2+} transporter

Greg M. Landry[1,2,3], Eva Furrow[6], Heather L. Holmes[1], Taku Hirata[1,2,3], Akira Kato[1,7], Paige Williams[1,2,3], Käri Strohmaier[1,2,3], Chris J.R. Gallo[1,3], Minhwang Chang[1], Mukesh K. Pandey[4], Huailei Jiang[4], Aditya Bansal[4], Marie-Christine Franz[1], Nicolas Montalbetti[1], Mariam P. Alexander[5], Pablo Cabrero[8], Julian A.T. Dow[8], Timothy R. DeGrado[4], Michael F. Romero [1,2,3,*]

[1]Physiology & Biomedical Engineering, [2]Nephrology & Hypertension, [3]O'Brien Urology Research Center, [4]Nuclear Medicine, [5]Laboratory Medicine & Pathology, Mayo Clinic College of Medicine, Rochester, MN 55905 USA; [6]Veterinary Clinical Sciences, College of Veterinary Medicine, University of Minnesota, St. Paul, Minnesota 55108, USA; [7]Center for Biological Resources and Informatics and Department of Biological Sciences, Tokyo Institute of Technology, Yokohama, Japan; [8]Institute of Molecular, Cell, and Systems Biology, College of Medical, Veterinary, and Life Sciences, University of Glasgow, Glasgow G12 8QQ, UK

**Correspondence to:*
Michael F. Romero, PhD, Physiology & Biomedical Engineering, Mayo Clinic College of Medicine, Rochester, MN 55905 USA; romero.michael@mayo.edu

Running Head: Renal ZIP10 localization in human, canine, and insect

ABSTRACT

Zinc (Zn^{2+}) is the second most abundant trace element, but is considered a micronutrient as it is a cofactor for many enzymes and transcription factors. While Zn^{2+} deficiency can cause cognitive immune or metabolic dysfunction and infertility, excess Zn^{2+} is nephrotoxic. As for other ions and solutes, Zn^{2+} is moved into and out of cells by specific membrane transporters: ZnT, Zip, and NRAMP/DMT proteins. ZIP10 is reported to be localized at the apical membrane of renal proximal tubules in rats, where it is believed to play a role in Zn^{2+} import. Renal regulation of Zn^{2+} is of particular interest in light of growing evidence that Zn^{2+} may play a role in kidney stone formation. The objective of this study was to show ZIP10 homologs transport Zn^{2+}, as well as ZIP10 kidney localization across species. We cloned ZIP10 from dog, human, and *Drosophila* (*CG10006*), tested clones for Zn^{2+} uptake in *Xenopus* oocytes, and localized the protein in renal structures. *CG10006*, rather than *foi* (fear-of-intimacy, *CG6817*) is the primary ZIP10 homolog found in *Drosophila* Malpighian tubules. The ZIP10 antibody recognizes recombinant dog, human and *Drosophila* ZIP10 proteins. Immunohistochemistry reveals that ZIP10 in higher mammals is found not only in the proximal tubule but also the collecting duct system. These ZIP10 proteins show Zn^{2+} transport. Together, these studies reveal ZIP10 kidney localization, a role in renal Zn^{2+} transport, and indicates that CG10006 is a *Drosophila* homolog of ZIP10.

Key words:
Slc39a10, kidney, *Xenopus* oocyte expression, PET isotope, immunohistochemistry

INTRODUCTION

Zn^{2+} is the second most biologically abundant trace element, following iron, is redox neutral and is an essential nutrient for nearly all organisms. The physiological importance of Zn^{2+} homeostasis is illustrated by its wide range of functions in the immune, endocrine, reproductive, skeletal, and neuronal systems and also due to the deleterious consequences of inherited diseases and severe zinc deficiencies (16, 19). Nonetheless, while Zn^{2+} has low toxicity (mM range), excess Zn^{2+} can be deleterious, e.g., causing inadequate copper absorption secondarily associated with sideroblastic anemia (2). Approximately 90% of zinc is stored in skeletal muscle and bone, with 5% in the liver and integument, and the remaining 2-3% in other tissues (16). Intestinal Zn^{2+} absorption is strictly regulated, increasing when dietary Zn^{2+} is limited, and decreasing via gastrointestinal secretion and renal excretion when in excess. As with all solutes requiring homeostasis, physiological Zn^{2+} levels are tightly controlled by specific, membrane-localized, Zn^{2+} import and export proteins.

Eukaryotic Zn^{2+} transporters are classified into two major families (19): Slc30 (ZnT, **Zin**c **T**ransporter) family (12) and Slc39 (Zip, **Z**rt-, **I**rt-like **p**rotein) family (13). Many studies indicate that the ZnT transporter family acts to decrease intracellular Zn^{2+} levels by transporting Zn^{2+} from the cytosol to the lumen of endosomes, vesicles, or secretory granules, then subsequently to the extracellular space, i.e., ZnT proteins are viewed as Zn^{2+} export transporters. By contrast, the Zip transporter family proteins are thought to increase intracellular, cytosolic Zn^{2+} levels by transporting Zn^{2+} either from the extracellular space or organellar lumen into the cytosol, i.e., Zip proteins are viewed as import transporters. In human and mammalian genomes,14 Zip transporter family members and 10 ZnT family members have been identified (20). Zn^{2+} can also be transported by macrophages and epithelia using the H^+ coupled divalent metal transporter DMT1 (NRAMP2) (22).

ZIP10 is regulated by external Zn^{2+} depletion or replenishment (15), cytokine signaling via the JAK/STAT pathway (23), and the metal-regulatory transcription factor 1 (MTF-1) (20). ZIP10 cloning and some functionality was reported initially in rat(15) and then mouse (29) (5). In these initial studies, investigators reasoned that rat ZIP10 can import Zn^{2+} into proximal tubule cells based on Zn^{2+} uptake by LLC-PK1 transfected with rat ZIP10. Pawan and coworkers showed that ZIP10-mediated Zn^{2+} uptake in rat renal and intestinal cells is regulated by thyroid hormones controlling overall cellular Zn^{2+} homeostasis (26). ZIP10 upregulation augments intracellular Zn^{2+} concentrations, a required cofactor for enzymes and transcription factors related to cell proliferation and could serve as a reparative response mechanism to kidney injury.

Additionally, Pal and colleagues reported a significant increase in ZIP10 expression in a highly aggressive renal cell carcinoma revealing ZIP10 quantification as an indicator of tumor aggressiveness (25). Our own preliminary work found in canine genome-wide association study (GWAS) that ZIP10 may be associated with calcium oxalate (CaOx) nephrolithiasis (8, 31). To better understand where and how ZIP10 might be associated with normal renal physiology and renal disease states, we sought to further elucidate the localization and functional details of ZIP10 in the kidney.

Transport proteins involved in Zn^{2+} movement within the renal tubular system, with the exception of rat, have not been well localized or characterized. In this study we report the cloning, function, and renal localization of SLC39A10 (ZIP10) from three species: human, dog, and fly. $^{63}Zn^{2+}$ uptake studies indicate that fly, dog and human clones transport Zn^{2+}, making them functional homologs of mouse and rat ZIP10. Currently, both dogs and flies are used as translatable models of CaOx nephrolithiasis. The current results will assist in explaining the role of Zn^{2+} and Zn^{2+} transport in the kidney.

MATERIALS AND METHODS

Animals and tissues. Flies (*Drosophila melanogaster*) were kept on standard medium or dietary salt substitution in vials at 22°C, 12:12 h photoperiod, and 40% relative humidity. Wild-type (Oregon R) and flies expressing the ZIP10 (CG10006) RNAi were used for cloning and RNAi-mediated experiments. Human cortical/medullary tissue was collected from non-neoplastic kidney tissue of patients distal to tumor by *at least* 2 cm. The IRB for Human Research (Mayo Clinic College of Medicine, Rochester, MN) approved these studies. Dog cortex/medullary kidney tissues were collected from control animals used in collaborative studies being performed within the Division of Cardiovascular Research. Addendums to animal protocols were approved by the IACUC (Mayo Clinic College of Medicine, Rochester, MN). *Xenopus* care and oocyte harvest were also IACUC approved. Both protocols are in accordance with the National Institutes of Health “Guide for the Care and Use of Laboratory Animals.”

Human, dog, and fly Slc39a10 (ZIP10) cloning. Full length cDNAs of human, and dog kidney Slc39a10, as well as whole fly body were amplified and inserted into the pGEMHE *Xenopus laevis* expression vector (21). All clones were obtained via PCR primer desin to the predicted starts and stops from the genomic DNA of the respective organisms. The resulting plasmids were linearized with *Not*I restriction enzyme and transcribed into cRNA *in vitro* using T7 RNA polymerase and mMESSAGE mMACHINE kits (Ambion, Austin, TX).

Oocyte isolation and injection. Xenopus laevis defolliculated oocytes were prepared as described previously (28) and injected with 50 nl of water (control) or human, dog, or fly cRNA at a concentration of 0.5 µg/µl (12.5 ng/oocyte) using a Nanoject-II injector (Drummond Scientific, Broomall, PA). Uptake and electrophysiology experiments were performed 2-4 days after injection.

^{63}Zn uptake studies. ^{63}Zn citrate in >99% radiochemical and radioisotopic purities was produced using a low energy cyclotron as previously described (6). The carrier medium for ^{63}Zn citrate was 2 mL sterile 4% sodium citrate. The ^{63}Zn citrate (~10.5 mCi) solution was diluted to 10 mL with 300 µl of stock solution defined below before addition to oocytes. Stock solutions were ND90 or ND96 (90 or 96 mM NaCl, 2 mM KCl, 1.8 mM $CaCl_2$, 1 mM $MgCl_2$, 5 mM HEPES, pH 7.5 or 8.5) with iso-osmotic ion replacements (choline chloride for 0Na, gluconate for 0Cl, bicarbonate for HCO_3^- ND90, and 90 mM KCl for K^+ ND90). Oocytes were pre-incubated with ND90, pH 7.5 for 20-30 min followed by 30 min uptake in above solutions containing ^{63}Zn-zinc citrate. The cells were then washed in ice cold ND90, pH 7.5 containing 1 mM nonradioactive $ZnCl_2$ to remove any nonspecific binding. ^{63}Zn uptake in each oocyte was determined by measurement of ^{63}Zn-radioactivity using a gamma counter, corrected for isotopic decay, and expressed as counts/min (CPM). Zinc uptake (nmol/h/oocyte) was calculated as ^{63}Zn uptake (CPM)/^{63}Zn administered (CPM). Uptake experiments were performed in duplicate with 10 oocytes in each experimental group for a total of 20 oocytes/group. Uptake data were log-transformed for statistical analysis to compare uptake between species and across solutions within each species. Statistical significance was determined by ANOVA followed by Tukey's test for pairwise comparisons implemented with R software for statistical computing (http://www.R-project.org/), and an adjusted p-value <0.05 was considered significant.

Electrophysiology and two-electrode voltage clamp. Electrophysiology protocols were performed as previously reported (30).

ZIP10 immunolocalization in oocytes. Oocytes were injected with either ZIP10 cRNA from all 3 species or water controls as described above. Immunolocalization was done as described previously (3). Sections were incubated with rabbit polyclonal IgG anti-ZIP10 (#6099; primary; ProSci Incorporated, Poway, CA) at 4ºC overnight, and allowed to incubate at RT with goat-anti-rabbit-AF568 (secondary). Cell nuclei were then stained with DAPI and ZIP10 surface staining was visualized via fluorescent microscopy with AF568 (red) and DAPI (blue) filters.

Cell type-specific knockdown of fly ZIP10. This was performed as described previously (11, 18). To specifically knockdown fly ZIP10, we used the CapaR-GAL4 driver (32), whereby the promoter of the tubule principal cell-specific gene neuropeptide Capa receptor drives GAL4 expression, and crossed it to a CG10006 fly line (101031: Vienna Drosophila Resource Center) possessing a transposable element directed against fly ZIP10.

Dog, fly, human, and mouse Slc39a10 (ZIP10) renal immunofluorescence. Malpighian tubules (MT) from female wild-type (Oregon R), as well as RNAi-mediated ZIP10 knockdown flies were dissected and transferred immediately to poly-L-lysine coated slides. Tubules were fixed in 4% paraformaldehyde/0.1% phosphate buffer for 1 h. Tubules were then incubated with anti-ZIP10 used above at 4ºC overnight. Tubules were incubated for 3 h at RT with goat-anti-rabbit-AF568. Tubules were stained with DAPI and visualized via fluorescent microscopy. The same ZIP10 antibody was used in mammalian tissues. Human, dog, and mouse cortical tissue samples were trimmed and fixed in 4% PFA/PBS for 1 h at 4°C. Tissue was placed in 10% (10 min), 16% (1h), and 18% (1h) sucrose/PBS solution. Immediately, tissue was placed in 20% sucrose/PBS overnight. The next day tissue was flash frozen, and embedded in OCT, and cryosections (10 µm) were prepared. For immunofluorescence, slides were allowed to rehydrate in PBS followed by blocking buffer incubation (10% donkey serum/1% BSA/PBST for ZIP10 and AQP2; 10% BlokHen (Aves Labs, Tigard, OR)/1% BSA/PBST for MCT-1). Slides were incubated overnight (4°C) with their primary antibodies/blocking buffer: ZIP10, MCT1, or AQP2 (chicken polyclonal IgY anti-MCT1, Chemicon, Billerica, MA; goat polyclonal IgG anti-AQP2, Novus Biologics, Littleton, CO). Slides were allowed to incubate with their secondary antibodies (Jackson ImmunoResearch, West Grove, PA): Cy3 (donkey-anti-rabbit), donkey-anti-chicken-AF647 (MCT-1), or

donkey-anti-goat-AF647 (AQP2) for 1 h at RT, and incubated with DAPI. ZIP10 fluorescence was visualized using Cy3 (red), and Alexa 647 for MCT-1 (green) and AQP-2 (yellow). For LTA (Lotus tetragonolobus agglutinin; Vector labs) we used a fluorescein-labeled version and incubated with slides during nthe secondary antibody application.

Western blotting. Kidneys from human, dog, and mouse were collected as described above and placed in ice-cold homogenization buffer containing 250 mM sucrose, 20 mM HEPES (pH 7.4 with HCl), 100 mM NaCl, 2 mM sodium EDTA, and homogenized using a PowerGen 125 (Fisher Scientific). The homogenate was centrifuged (15 min at 1150 x g, 5424 R centrifuge (Eppendorf)) at 4°C. The pellet (P1) containing debris and nuclei was discarded, and previous step was repeated a second time. The resultant supernatant (S1) was centrifuged (30 min at 20,000 x g, 5424 R centrifuge (Eppendorf)) at 4°C, and the supernatant (S2) was discarded. The resulting microsomal pellet (P2) containing plasma and organellar membranes was resuspended in homogenization buffer, assayed for protein content (Bradford assay), and stored at -20°C. 0.6 µg of protein were loaded into each well, and western blotting was performed using a WES Simple Western automated immunoblot system (ProteinSample, San Jose, CA) according to the manufacturer's instructions. The same rabbit polyclonal IgG anti-ZIP10 antibody (as above) utilized in the immunolocalization studies mentioned above was utilized to perform Western blots.

RESULTS

Protein comparison of human(h), dog(d), mouse(m), and Drosophila (fly, CG10006) Slc39a10(ZIP10).

To highlight *SLC39A10* (i.e., ZIP10) as a gene of interest in kidney stone disease, (8, 31) ENREF 22 we cloned the ZIP10-cDNA for dog (KY094513) and human ZIP10 (NM_001127257) (**Figure 1A**). Two genes, *foi*/*CG6817* and *dZip71B*/*CG10006* were identified as the closest *Drosophila* orthologues (34) (http://flybase.org/reports/FBgn0036461.html) (**Figure 1B)**. Pileup analysis (**Figure 1B**) shows that there are multiple blocks of identity between the human, dog and mouse ZIP10 cDNAs and *CG10006*. Divergence analysis indicates that *CG10006* is ~30% identical to the 3 mammalian cDNAs (**Figure 1B**). However, data available in FlyAtlas (http://flyatlas.org/atlas.cgi) revealed that *CG6817* (i.e., *fear of intimacy*, *foi*) has low expression in Malpighian tubules (MT, fly renal structures): larval MT (95±1) and adult MT (95±1). Whereas, *CG10006* is expressed almost exclusively in the tubules (**Figure 1C**) at high levels: larval MT (3219±48) and adult MT (902±145). Thus CG10006 was better suited for evaluation of renal Zn^{2+} handling in flies.

^{63}Zinc transport by human, dog, and fly Slc39a10(ZIP10).

Xenopus oocytes were injected with SLC39A10 cRNAs (copy RNAs) from each species, using water as a control. Three days after cRNA injection, we performed 30 min $^{63}Zn^{2+}$ uptake incubations. All 3 clones showed a significant increase in $^{63}Zn^{2+}$ uptake compared to water-injected controls (**Figure 2A**), with fly ZIP10 (CG10006) showing an 8-fold increase, hZIP10 showing a 5 fold increase, and dZIP10 showing a 7 fold increase (nmol/h/oocyte: water, 0.47; fly ZIP10, 3.81; hZIP10, 2.47; dZIP10, 3.04). Thus, fly ZIP10, hZIP10 and dZIP10 all transport Zn^{2+}. Interestingly, fly ZIP10 transported significantly more Zn^{2+} than human ZIP10 (**Figure 2A).**

Since hZIP2 and ZIP8 were previously reported as a Zn^{2+}/HCO_3^- cotransporter (9), we tested if ZIP10 might be pH- or HCO_3^- dependent. Starting solution was a pH 7.5 NaCl-ringer (see Methods). Adjusting solution pH to 8.5 did not change uptake for any clone. Since we did not want to bubble our $^{63}Zn^{2+}$ solutions with CO_2 (to maintain pH 7.5), we replaced NaCl and KCl with $NaHCO_3$ and $KHCO_3$. This resulted in a solution pH of ~8.5 (so the non-HCO_3^- solution was 8.5). This pH8.5-HCO_3 solution did not significantly alter uptake for any clone **(Figure 2B)**. Combined these data indicate that high pH does not affect transport for ZIP10. These data do not support that ZIP10 operates as a Zn^{2+}/HCO_3^- cotransporter.

To further determine the ionic coupling of ZIP10, we performed ion-replacements during $^{63}Zn^{2+}$ uptake. Replacement of Na^+ with choline or Cl^- with gluconate did not change uptake (**Figure 2B**). Depolarization (7.5, KCl) also did not alter $^{63}Zn^{2+}$ uptake.

Intracellular pH (pH_i) and cellular currents

To more directly determine if Zn^{2+} would change pH_i with and with out HCO_3^-, we measure pH_i in ZIP10 expressing oocytes (**Figure 3A-C**). **Figure 3A** shows that addition of 1 mM Zn without or with 33 mM HCO_3^-, does not elicit a pH_i change. **Figure 3B, C** show the experiments except that the ZIP10 oocytes are also

voltage clamped. When clamping the oocyte, Zn^{2+} also does not elicit a current or change pH_i. Finally, voltage steps with the addition of 1 mM or 5 mM Zn^{2+} does not reveal a voltage dependent current (**Figure 3D**).

Human, dog, mouse, and Drosophila (fly) Slc39a10 (ZIP10) tissue localization.

ZIP10 has only been localized to rodent kidney (15). An anti-ZIP10 antibody was raised against an 18 amino acid synthetic peptide near the center of human ZIP10; however, the exact peptide is not revealed by the manufacturer. Thus, before staining renal tissue from other animals, we determined if the ZIP10 antibody would recognize recombinant ZIP10 protein expressed in *Xenopus* oocytes (**Figure 4**). Oocytes were injected with water (**Figure 4A,** control), dog ZIP10 (**Figure 4B**), human ZIP10 (**Figure 4C**) and *Drosophila* CG10006 (**Figure 4D**). Dog, human and *Drosophila* membrane protein was recognized by the ZIP10 antibody, whereas the water-injected controls showed no ZIP10 staining (**Figure 4A**) indicating that the ZIP10 antibody recognizes dog SLC39A10 protein, human SLC39A10 protein and the *Drosophila* CG10006 protein. To verify that our aliquots of the commercial ZIP10-antibody recognized the correct sized protein, we preformed Western analysis (WES) using kidney homogenates of mouse, dog and human kidney (**Figure 5**). These blots show immunoreactivity of a 94 kD protein which is the predicted size of ZIP10 in all three species (**Figure 5A**). To normalize for protein loading, a ratio against β-actin was done (**Figure 5B**).

Since ZIP10 has been previously localized in rat kidney and out ZIP10 antibody recognizes the correct protein, we initially localized ZIP10 in the mouse kidney (**Figure 6**). Immunofluorescence of mouse kidney sections illustrates that the ZIP10-antibody recognizes protein at the apical membrane of the proximal tubule. Monocarboxylate transporter-1 (MCT1, Slc16a1) is specific to the basolateral membrane of the proximal tubule and is colocalized with ZIP10 reactivity (**Figure 6A**). Aquaporin-2 (AQP2) counterstaining, collecting duct (CD) marker, revealed no colocalization with Zip10 reactivity in mouse (**Figure 6B)**. LTA, a proximal tubule glycocalyx marker, colocalized with Zip10 while uromodulin (UROD), a marker of the thick ascending limb (TAL), did not (**Figure 6C**). These colocalization studies clearly indicate that Zip10 is found predominantly at the apical membranes of proximal tubules in the mouse kidney. Colocalization of Zip10 with LTA and AQP2, also illustrates that Zip10 seems exclusively proximal tubule in mouse (**Figure 6D**).

Figure 4D shows that the ZIP10 antibody recognizes the recombinant *Drosophila* CG10006 (fly ZIP10) protein with ZIP10-reactivity ubiquitously expressed along the MT-luminal border (**Figure 7A**). To further test the ZIP10-antibody specificity, we used a MT-principal cell specific ZIP10 knockdown (CapaR-GAL4: UAS-CG10006-RNAi). **Figure 7B** shows no MT-luminal staining in these CG10006-knockdown MTs, further indicating ZIP10-antibody recognition of the CG10006 protein in *Drosophila*. Recognition of recombinant ZIP10 from all 4 species (**Figure 4**) indicates evolutionary conservation of this protein across species. These data further indicate CG10006 as a *Drosophila* homolog of ZIP10 with similar renal expression to that of mouse.

Knowing that the ZIP10-antibody recognizes the recombinant proteins, we sought to determine if dog and human ZIP10 protein localization was similar to that of mouse and fly. Both dog (**Figure 8A**) and human (**Figure 9A**) kidney displayed ZIP10 proximal tubular apical reactivity confirmed with MCT1 colocalization. However, dog and human non-proximal tubules appeared immunoreactive (**Figure 8A, Figure 9A**). Unfortunately, LTA does not seem to react with dog kidney glycocalyx (not shown), so we examined NKCC2 and UMOD localization with ZIP10 in cortex (**Figure 8B**) and medulla (**Figure 8C)**. NKCC2 and UMOD colocalize but there is little if any localization with ZIP10 in dog. Colocalization staining with AQP2 indicates cortical collecting duct colocalization in dog (**Figure 8D-F**) with apical ZIP10 expression. In human kidney, ZIP10 localizes with MCT1 but not NKCC2 (**Figure 9B**), LTA labels PT apical membranes and colocalizes with ZIP10 in human (**Figure 9C**), but ZIP10 does not localize with UROD (**Figure 9C**). As with dog kidney, ZIP10 shows obvious colocalization with AQP2 in human kidney indicating robust protein expression in collecting duct. Both **Figure 8** and **Figure 9** illustrate dog and human ZIP10 extending beyond the proximal nephron; prominently in the cortical collecting duct (see cartoon in **Figure 10**).

Together our results indicate that these three mammalian species all express ZIP10, and that it is localized prominently on the apical membrane of the proximal tubule (mouse (**Figure 6A**), dog (**Figure 8A**) and human (**Figure 9A**)). Furthermore, dog (Error! Reference source not found.**D**) and human (**Figure 9D**) ZIP10 protein is in cortical collecting ducts, indicating ZIP10 expression beyond the proximal tubule in higher order mammals (**Figure 10**).

DISCUSSION

Zinc homeostasis is controlled by Zn^{2+} export and import proteins. These distinct transporter groups are encoded by three solute-linked carrier (*Slc*) gene families: Zip (*Slc39*; importers)(13); ZnT (*Slc30*; exporters) (26); (12) and DMT / NRAMP proteins (Slc11 H^+ coupled divalent metal transporters) (22, 24). Zip transporters increase cytosolic Zn^{2+} availability by facilitating extracellular Zn^{2+} uptake, as well as vesicular Zn^{2+} release into the cytosol (13). In contrast, ZnT transporters reduce cytosolic Zn^{2+} availability by facilitating Zn^{2+} efflux into the extracellular environment or intracellular vesicles (12). DMT1 / NRAMP2 is a general H^+ coupled transition metal transporter, localized to apical epithelial membranes, and is involved in divalent metal uptake (Fe^{2+}>Zn^{2+}>Cd^{2+}, Ni^{2+}, Co^{2+}) into cells or intracellular compartments (10, 22).

ZIP10 has been studied in various murine cell types and organ systems including erythrocytes (29), testicles (5), liver and brain (20), the immune system (B cell development) (23), and oocytes (17). ZIP10 is suggested as involved in human breast cancer metastasis and invasiveness (14) as well as renal cell carcinoma aggressiveness (25). However, ZIP10 expression, function, and localization in renal tubular systems are not well understood, and ZIP10 has only been characterized in rat brush border membranes (BBM). Functional data from this system suggests rat ZIP10 mRNA expression is regulated by zinc levels, as well as functions to import Zn^{2+} across the rat renal BBM (15). Kaler and Prasad reported that *SLC39A10* was abundantly expressed in human kidney, but did not specify precise tissue localization (15). While human ZIP10 has been used as a cancer marker (7), its function and localization in the human kidney has not been explored. Furthermore, no information has been previously reported for dog ZIP10.

Comparatively, two *Drosophila* homologs identify with mammalian ZIP10, *CG10006* and *CG6817* (*foi*). **Figure 1B, D** illustrate that *foi* is less divergence from mammalian and other ZIP10 proteins (34) and based on molecular sequence distances has been designated as Zip6 or ZIP10 (27, 34). However, *foi* has relatively low expression in fly renal tubules (MTs), whereas ZIP10 has moderate to high renal expression in mammals (http://proteinatlas.org). In contrast, *CG10006* is enriched in MTs (**Figure 1C**). Since our interest was in renal Zn^{2+} transport, we focused on *CG10006*.

Step one is to determine transporter protein localization on the tissue level, cell type, and intracellularly. This study used immunohistochemistry to investigate ZIP10 localization in mouse, dog, and human kidney, as well as *Drosophila* MTs. **Figure 4 - 9** illustrate that ZIP10 from these four species are detected with the ZIP10 antibody. Not surprisingly, mouse ZIP10, like rat ZIP10 (15), is localized predominantly on the apical membrane of the proximal tubule without any detection elsewhere in the kidney (**Figure 6A).** While it is not surprising that mammalian ZIP10 is found in the apical membrane of the proximal tubule, staining of dog and human kidney indicates that ZIP10 is also found in other renal cortical regions, particularly the cortical collecting duct (CCD) (**Figure 8B; 9B**). Dog and human CCD ZIP10 localization could indicate a final re-absorptive process facilitating Zn^{2+} movement from the CCD lumen into the peritubular capillaries, especially as a mechanism to maintain Zn^{2+} homeostasis in Zn^{2+} deficient states.

Hypothetically, rodents should possess the same mechanism for Zn^{2+} reabsorption in distal nephron segments. Li and coworkers have reported ZIP10 mRNA in mouse DCT cells (33). However, these cell-line mRNA results are not supported by ZIP10 immunolocalization in mouse kidney. The results here indicate that there are distinct differences in rodents versus dog and human kidney localization, and presumably physiology. It is attractive to speculate that such a difference may contribute to rodents being very resilient to forming kidney stones. Nevertheless, this speculation may be difficult to test and requires further investigation.

Moreover, CG10006, while only 30% identical to mammalian ZIP10 is immunologically related and found in the apical membrane of adult MTs (**Figure 7A**). Although this differs from a basolateral location reported in larvae (35), this could reflect a difference in insect Zn^{2+} requirements especially since there was significant Zn^{2+} uptake compared to hZIP10, thus suggesting a role for ZIP10 across metamorphosis. . *Drosophila* Zip10 localization in our studies is specific to MT principal cells, as the CapaR-CG10006-RNAi removes immunoreactivity (**Figure 7B**). These data indicate that *CG10006* is a ZIP10 homolog in *Drosophila* and suggest evolutionary conservation of renal-localized Zn^{2+} transport proteins between invertebrates and vertebrates.

Our studies directly tested ZIP10 clone Zn^{2+} transport function by expressing these proteins in *Xenopus* oocytes. We originally tried to assay ZIP10 function using Zn-selective microelectrodes as we have previously done for pH, Na^+, Cl^-, K^+ and NH_4^+. As Zn^{2+} is divalent the maximum, ideal-electrode response is 30 mV/decade [Zn^{2+}]. Calibration of the Zn^{2+} ionophore revealed that its response was ~20 mV/ decade [Zn^{2+}], making it very difficult to use for quantification. These experiments did reveal that addition of even 5 mM Zn^{2+} to oocyte bathing solutions did not cause voltage nor current changes. Nonetheless, these experiments indicated that ZIP10 proteins are electroneutral. Using two-electrode voltage clamp with human ZIP10 resulted

in no current stimulated by addition of Zn^{2+}. Moreover, intracellular pH (pH_i) measurements revealed that in the presence and absence of HCO_3^-, Zn^{2+} addition did not change pH_i. These results corroborate previous studies which have shown that the similar ZIP transporter, ZIP2, also does not transport HCO_3^- (36). These data indicate that Zn^{2+}:HCO_3^- cotransport is unlikely to occur through ZIP10.

We directly assessed Zn^{2+} transport using Zn^{2+} isotopic uptake. Since $^{63}Zn^{2+}$ is a short-lived PET isotope ($t_{0.5}$ = 38.5 min), we could perform uptake measurements for short durations and maintain high specific activity. Our experiments clearly show that Zn^{2+} is transported by all the ZIP10 clones **Figure 2A**. Eide is the only one to propose a transport mechanism for any of the mammalian Zip proteins (9). To elucidate the mechanism of ZIP10 transport, we tested the role of OH^- and HCO_3^- on Zn^{2+} transport (**Figure 2B, Figure 3**). These experiments illustrate that neither elevated extracellular pH nor HCO_3^- stimulate Zn^{2+} transport. Moreover, if pH_i is measure, Zn^{2+} does not elicit a pH_i change (**Figure 3A-C**); and voltage clamping indicates that there are no Zn^{2+} evoke currents (**Figure 3B-D**). Therefore, in contrast to Zip2, ZIP10 protein activities are not enhanced. Replacement of Na^+ and Cl^- also did not affect Zn^{2+} uptake (**Figure 2B**). Thus, these experiments do not provide a discrete model of the mechanism of Zn^{2+} transport, but rather support the general conclusion that all ZIP10 clones transport Zn^{2+} as their substrate, regardless of species.

While it is attractive to speculate that renal ZIP10-mediated Zn^{2+} transport is identical among mammals, ZIP10 protein appears more widespread in dog and human kidney compared to rat and mouse kidney (**Figure 10**). Without knowing ionic coupling or solute gradients, it is difficult to predict if proximal tubule and CCD ZIP10-mediated Zn^{2+} movements are in the same uptake or export direction. Perhaps additional distal nephron Zip transporters enable additional control of systemic Zn^{2+}. This study does establish that CG10006 is the ZIP10-fly homolog, ZIP10 proteins are Zn^{2+} transporters, and that ZIP10 in human kidney is expressed beyond the proximal tubule. ZIP10's role in the CCD remains to be elucidated.

Acknowledgements.

We thank Jessica Busch for excellent technical assistance. We thank Adam J. Rossano for help optimizing imaging and comments on the manuscript. This work was supported by NIH grants: DK092408, U54-DK100227 (O'Brien Urology Research Center) and R25-DK101405 and a grant from the Oxalosis & Hyperoxaluria Foundation. GML was supported by T32-DK007013.

Contributions.

GML, EF, TH, PC, JATD and MFR conceived experiments, designed experimental protocols and drafted the manuscript.

TH cloned and sequenced human SLC39A10, canine Slc39a10 and *Drosophila* CG10006.

PC and JATD aided in cloning CG10006.

MKP, HJ, BA and TRD made and purified the $^{63}Zn^{2+}$.

GML, EF, TH, PW, KS, CJRG, MCF, NM and MFR carried out the $^{63}Zn^{2+}$ uptake experiments.

GML, HLH, TH and AK performed immunohistochemistry and MPA accessed ZIP10 localization in human kidney. TH, NM, MC and MFR performed electrophysiology experiments.

GML, HLH, EF and MFR assembled and proofed the manuscript and figures.

Figure Legends

Figure 1. Slc39a10 sequence analyses.
(A) Sequence pileup of human SLC39A10 (H; NM_001127257), dog slc39a10 (D; KY094513), mouse (M; NP_76624), and *Drosophila* (CG10006; dZip71B, fly ZIP10). Human, dog, mouse and *Drosophila* ZIP10 cDNAs were amplified from kidney (human, dog, and mouse) or whole body (fly) by RT-PCR using gene-specific primers based on 5' and 3' expressed sequence tag primers. Black shading indicates identical amino acids in all 4 (human, dog, mouse, and fly) gene products, whereas grey shading indicates similar functional groups. **(B)** identity and divergence analysis of ZIP10 clones**. (C)** Distribution of CG10006 mRNA in larval (left) and adult (right) Drosophila. Data are mined from FlyAtlas.org, an Affymetrix microarray-derived expression atlas of *Drosophila* (4).

Figure 2. $^{63}Zn^{2+}$ uptake by ZIP10 clones in *Xenopus laevis* oocytes expressing recombinant human, dog, or Drosophila ZIP10.
(A) *Xenopus laevis* oocytes injected with cRNA coding for either human, dog, or fly (*Drosophila)* ZIP10 (Slc39a10) and water controls were used for $^{63}Zn^{2+}$ uptake. The data from the pH 7.5 uptake solution is shown in panel A. All species had significant uptake ($p < 0.001$) compared to water and no interspecies differences were detected ($p > 0.05$), as determined by ANOVA with Tukey's post-hoc test. **(B)** The same four groups of oocytes were placed in 6 different solutions with varying iso-osmotic ion replacements, and $^{63}Zn^{2+}$ uptake was measured in nmol/ho/oocyte; n = 10 oocytes per solution done in 2 replicates with a total n = 120 oocytes per species. Log-scaled data are shown. *Xenopus laevis* oocytes injected with cRNA coding for either human, dog, or fly (Drosophila) ZIP10 (Slc39a10) were placed in either pH 7.5 ND90/96 (black), pH 8.5 ND90/96, pH 8.5 HCO3-, pH 7.5 0mM Na+, pH 7.5 0mM Cl-, or pH 7.5 KCl (high potassium), and $^{63}Zn^{2+}$ uptake was measured in nmol/ho/oocyte; n = 10 oocytes per solution done in 2 replicates. Log-scaled data are shown. $^{63}Zn^{2+}$ uptake did not differ significantly between solutions for any species ($p > 0.05$), as determined by ANOVA with Tukey's post-hoc test.

Figure 3. Electrophysiology characterization of ZIP10 in *Xenopus* oocytes
Xenopus oocytes were injected with human ZIP10 cRNA. (A) shows a non-voltage clamped experiment in which intracellular pH (pH_i) and membrane potential (V_m) were measure, and 1mM $ZnCl_2$ (blue shading) added in the absence or presence of 5% CO_2/ 33 mM HCO_3^- (pH 7.5; tan shading). (B) and (C) show similar experiments in which pH_i is measured while the oocytes is clamped at -20 mV. (D) Current-Volatge (IV) curves of ZIP10 oocytes with 0 mM Zn^{2+} (ND96), 1 mM Zn^{2+} and 5 mM Zn^{2+} . The red-dotted circle indicates an air bubble in the system which also manifest as a quick current spike. The repeat maneuver shows no pH_i or current change.

Figure 4. Human, dog, and *Drosophila* ZIP10 expression in *Xenopus* oocyte plasma membrane.
Xenopus laevis oocytes were injected with cRNA coding for either water (**A**, control), dog ZIP10 (**B**), human ZIP10 (**C**), or dZIP10 (**D**, CG10006). To determine if a commercial available ZIP10 antibody would detect, the expressed Zip-proteins, oocytes were processed immunohistochemistry 3-5 days after cRNA injection. Fluorescent immunohistochemistry shows recognition of recombinant protein epitopes across species (Red: human, dog, and fly), but not water-injected control. DAPI denotes cell interior as counterstain (blue). Magnification at 20x.

Figure 5. ZIP10 (Slc39A10) expression in normal mouse, dog, and human kidney.
Left: Immunoblot analysis of ZIP10 expressions in kidneys from normal mouse, dog, and human tissue. The apparent molecular mass for mouse, dog, and human ZIP10 (94 kDa) is the same across species, and matches the reported weight recognized by the rabbit polyclonal antibody. *Right:* Graphical representation of ZIP10 protein levels normalized to β-actin loading controls.

Figure 6. Immunofluorescent detection of mouse ZIP10 (Slc39a10).
(A) Immunofluorescence of mouse kidney section co-stained with Zip10 (red) and monocarboxylate transporter-1 (MCT1; green; basolateral membrane of PT). Note there is additional apical Zip10 staining**. (B)** Immunofluorescence of a mouse kidney section co-stained with Zip10 (red) and aquaporin-2 (AQP2; yellow; apical membrane of collecting duct (CD))**.** DAPI denotes proximal tubule cell nuclei (blue). (**C**) Mid-cortical section of mouse kidney stained with Zip10 (red), LTA (green; glycocaylx of PT) and uromodulin (UMOD or

Tamm Horsfall; white; Thick ascending limb (TAL)). (D) cortical section of mouse kidney stained with Zip10 (red), LTA (green; glycocaylx of PT). Bars are 100 µm.

Figure 7. Immunofluorescent detection of ZIP10 in the *Drosophila* Malpighian Tubule.
(**A**) Immunohistochemistry showing specific labeling of ZIP10 (red) in the MT lumen in an ORWT female, anterior MT. (**B**) When CG10006-RNAi is driven by CapaR-Gal4 (MT principal cells), there is no specific labeling with the ZIP10-antibody which does recognize the *Drosophila* epitope (**Figure 3D**). DAPI denotes principal and stellate cell nuclei (blue). Magnification at 20x.

Figure 8. Immunofluorescent detection of ZIP10 (Slc39a10) in normal dog kidney.

(A) Immunofluorescence showing specific labeling of dog ZIP10 (red) on the apical membrane of proximal tubule (PT) cells colocalized with monocarboxylate transporter-1 (MCT1) (green; basolateral membrane. (**B**) is a cortical section of dog kidney costained with Zip10 (red), NKCC2 (green, apical, TAL) and UMOD (white; TAL). (**C**) is a near-medullary section of dog kidney costained with Zip10, NKCC2 and TammHf showing clear TAL segments. (**D**) Immunofluorescence colocalizing ZIP10 with aquaporin-2 (AQP2; yellow) marking the apical membrane of collecting duct (CD) cells. **E** and **F** show ZIP10 and AQP2 alone, respectively, from panel **D**. DAPI denotes cell nuclei (blue). Bar = 100 µm

Figure 9. Immunofluorescent detection of ZIP10 (SLC39A10) in normal, adult human kidney.
Immunofluorescent staining of normal human kidney sections. The white bar in each panel is 100 µm. (**A**) shows co-staining of ZIP10 (red), MCT1 (green; PT) and DAPI. Obviously co-stained PT's are indicated. (**B**) shows co-staining using ZIP10 (red), MCT1 (green; PT) and NKCC2 (white; TAL). (**C**) shows co-staining using ZIP10 (red), LTA (green; PT) and UMOD (white; TAL). (**D**) as in Figure 8 (dog kidney) shows co-localization of ZIP10 (red) and AQP2 (yellow; CD) in some but not all tubules. DAPI denotes cell nuclei (blue).

Figure 10. Nephron cartoon summarizing differences between mouse and dog / human Zip10 staining
Two nephron diagrams showing Zip10 reactivity: mouse (left) and dog or human (right). The thick red line indicates tubule areas where ZIP10 protein staining was found.

References

1. **Bin BH, Bhin J, Takaishi M, Toyoshima KE, Kawamata S, Ito K, Hara T, Watanabe T, Irie T, Takagishi T, Lee SH, Jung HS, Rho S, Seo J, Choi DH, Hwang D, Koseki H, Ohara O, Sano S, Tsuji T, Mishima K, and Fukada T**. Requirement of zinc transporter ZIP10 for epidermal development: Implication of the ZIP10-p63 axis in epithelial homeostasis. *Proceedings of the National Academy of Sciences of the United States of America* 2017.
2. **Broun ER, Greist A, Tricot G, and Hoffman R**. Excessive zinc ingestion. A reversible cause of sideroblastic anemia and bone marrow depression. *JAMA : the journal of the American Medical Association* 264: 1441-1443, 1990.
3. **Chen AP, Chang MH, and Romero MF**. Functional analysis of nonsynonymous single nucleotide polymorphisms in human SLC26A9. *Human Mutation* 33: 1275-1284, 2012.
4. **Chintapalli VR, Wang J, and Dow JA**. Using FlyAtlas to identify better Drosophila melanogaster models of human disease. *Nat Genet* 39: 715-720, 2007.
5. **Croxford TP, McCormick NH, and Kelleher SL**. Moderate zinc deficiency reduces testicular Zip6 and ZIP10 abundance and impairs spermatogenesis in mice. *The Journal of nutrition* 141: 359-365, 2011.
6. **DeGrado TR, Pandey MK, Byrne JF, Engelbrecht HP, Jiang H, Packard AB, Thomas KA, Jacobson MS, Curran GL, and Lowe VJ**. Preparation and preliminary evaluation of 63Zn-zinc citrate as a novel PET imaging biomarker for zinc. *Journal of nuclear medicine : official publication, Society of Nuclear Medicine* 55: 1348-1354, 2014.
7. **Franz MC, Anderle P, Burzle M, Suzuki Y, Freeman MR, Hediger MA, and Kovacs G**. Zinc transporters in prostate cancer. *Molecular aspects of medicine* 34: 735-741, 2013.
8. **Furrow E, Mickelson J, Lulich JP, Armstrong P, Minor K, and Patterson E**. Metabolic and genetic determinants of calcium oxalate urolithiasis in dogs. *J Vet Intern Med* 28: 1365, 2014.
9. **Gaither LA, and Eide DJ**. Functional expression of the human hZIP2 zinc transporter. *J Biol Chem* 275: 5560-5564, 2000.
10. **Gunshin H, Mackenzie B, Berger UV, Gunshin Y, Romero MF, Boron WF, Nussberger S, Gollan JL, and Hediger MA**. Cloning and characterization of a mammalian proton-coupled metal-ion transporter. *Nature* 388: 482-488, 1997.
11. **Hirata T, Cabrero P, Bondeson DP, Berkholz DS, Thompson JR, Ritman E, Dow JAT, and Romero MF**. *In vivo Drosophila* model for calcium oxalate nephrolithiasis. *Am J Physiol Renal Physiol* 303: F1555-1562, 2012.
12. **Huang L, and Tepaamorndech S**. The SLC30 family of zinc transporters - A review of current understanding of their biological and pathophysiological roles. *Molecular aspects of medicine* 34: 548-560, 2013.
13. **Jeong J, and Eide DJ**. The SLC39 family of zinc transporters. *Molecular aspects of medicine* 34: 612-619, 2013.
14. **Kagara N, Tanaka N, Noguchi S, and Hirano T**. Zinc and its transporter ZIP10 are involved in invasive behavior of breast cancer cells. *Cancer Sci* 98: 692-697, 2007.
15. **Kaler P, and Prasad R**. Molecular cloning and functional characterization of novel zinc transporter rZIP10 (Slc39a10) involved in zinc uptake across rat renal brush-border membrane. *American journal of physiology Renal physiology* 292: F217-229, 2007.
16. **Kambe T, Tsuji T, Hashimoto A, and Itsumura N**. The Physiological, Biochemical, and Molecular Roles of Zinc Transporters in Zinc Homeostasis and Metabolism. *Physiological reviews* 95: 749-784, 2015.
17. **Kong BY, Duncan FE, Que EL, Kim AM, O'Halloran TV, and Woodruff TK**. Maternally-derived zinc transporters ZIP6 and ZIP10 drive the mammalian oocyte-to-egg transition. *Molecular human reproduction* 20: 1077-1089, 2014.
18. **Landry GM, Hirata T, Anderson JB, Cabrero P, Gallo CJR, Dow JAT, and Romero MF**. Sulfate and thiosulfate inhibit oxalate transport via a dPrestin (mSlc26a6)-dependent mechanism in an insect model of calcium oxalate nephrolithiasis. *Am J Physiol Renal Physiol* 310: F152-159, 2016.
19. **Lichten LA, and Cousins RJ**. Mammalian zinc transporters: nutritional and physiologic regulation. *Annu Rev Nutr* 29: 153-176, 2009.

20. **Lichten LA, Ryu MS, Guo L, Embury J, and Cousins RJ**. MTF-1-mediated repression of the zinc transporter ZIP10 is alleviated by zinc restriction. *PloS one* 6: e21526, 2011.
21. **Liman ER, Tytgat J, and Hess P**. Subunit stoichiometry of a mammalian K+ channel determined by construction of multimeric cDNAs. *Neuron* 9: 861-871, 1992.
22. **Mackenzie B, Ujwal ML, Chang M-H, Romero MF, and Hediger MA**. Divalent metal-ion transporter DMT1 mediates both H^+-coupled Fe^{2+} transport and uncoupled fluxes. *Pflugers Arch* 451: 544 - 558, 2006.
23. **Miyai T, Hojyo S, Ikawa T, Kawamura M, Irie T, Ogura H, Hijikata A, Bin BH, Yasuda T, Kitamura H, Nakayama M, Ohara O, Yoshida H, Koseki H, Mishima K, and Fukada T**. Zinc transporter SLC39A10/ZIP10 facilitates antiapoptotic signaling during early B-cell development. *Proceedings of the National Academy of Sciences of the United States of America* 111: 11780-11785, 2014.
24. **Montalbetti N, Simonin A, Kovacs G, and Hediger MA**. Mammalian iron transporters: Families SLC11 and SLC40. *Molecular aspects of medicine* 34: 270-287, 2013.
25. **Pal D, Sharma U, Singh SK, and Prasad R**. Association between ZIP10 gene expression and tumor aggressiveness in renal cell carcinoma. *Gene* 552: 195-198, 2014.
26. **Pawan K, Neeraj S, Sandeep K, Kanta Ratho R, and Rajendra P**. Upregulation of Slc39a10 gene expression in response to thyroid hormones in intestine and kidney. *Biochimica et biophysica acta* 1769: 117-123, 2007.
27. **Richards CD, and Burke R**. A fly's eye view of zinc homeostasis: Novel insights into the genetic control of zinc metabolism from Drosophila. *Archives of biochemistry and biophysics* 611: 142-149, 2016.
28. **Romero MF, Fong P, Berger UV, Hediger MA, and Boron WF**. Cloning and functional expression of rNBC, an electrogenic Na^+-HCO_3^- cotransporter from rat kidney. *Am J Physiol* 274: F425-432, 1998.
29. **Ryu MS, Lichten LA, Liuzzi JP, and Cousins RJ**. Zinc transporters ZnT1 (Slc30a1), Zip8 (Slc39a8), and ZIP10 (Slc39a10) in mouse red blood cells are differentially regulated during erythroid development and by dietary zinc deficiency. *The Journal of nutrition* 138: 2076-2083, 2008.
30. **Sciortino CM, and Romero MF**. Cation and voltage dependence of rat kidney, electrogenic Na^+/HCO_3^- cotransporter, rkNBC, expressed *in* oocy*tes. Am J Physiol* 277: F611-623, 1999.
31. **Strohmaier K, Williams P, Hirata T, Cabrero P, Dow JA, Furrow E, and Romero MF**. Zn^{2+} and ZIP10 knockdown alter *in vivo* and *ex vivo* calcium oxalate (CaOx) crystal formation in *Drosophila* stone model. *J Am Soc Nephrol* 25: 647A, 2014.
32. **Terhzaz S, Cabrero P, Robben JH, Radford JC, Hudson BD, Milligan G, Dow JA, and Davies SA**. Mechanism and function of Drosophila capa GPCR: a desiccation stress-responsive receptor with functional homology to human neuromedinU receptor. *PloS one* 7: e29897, 2012.
33. Li MS, Adesina SE, Ellis CL, Gooch JL, Hoover RS, Williams CR. NADPH oxidase-2 mediates zinc deficiency-induced oxidative stress and kidney damage. *Am J Physiol Cell Physiol*. 312(1): C47-C55, 2017.
34. **Xiao G, and Zhou B**. What can flies tell us about zinc homeostasis? *Archives of biochemistry and biophysics* 611: 134-141, 2016.
35. **Yin S, Qin Q, and Zhou B**. Functional studies of Drosophila zinc transporters reveal the mechanism for zinc excretion in Malpighian tubules. *BMC Biol* 15: 12, 2017.
36. Franz MCT, Pujol-Giménez J, Montalbetti NT, Fernandez-Tenorio M, Niggli E, Romero MF, and Hediger MA. Reassessment of the Transport Mechanism of the Human Zinc Transporter SLC39A2. *Biochemistry 57 (26): 3976-3986, 2018. DOI: 10.1021/acs.biochem.8b00511. PMID 29791142*.

A

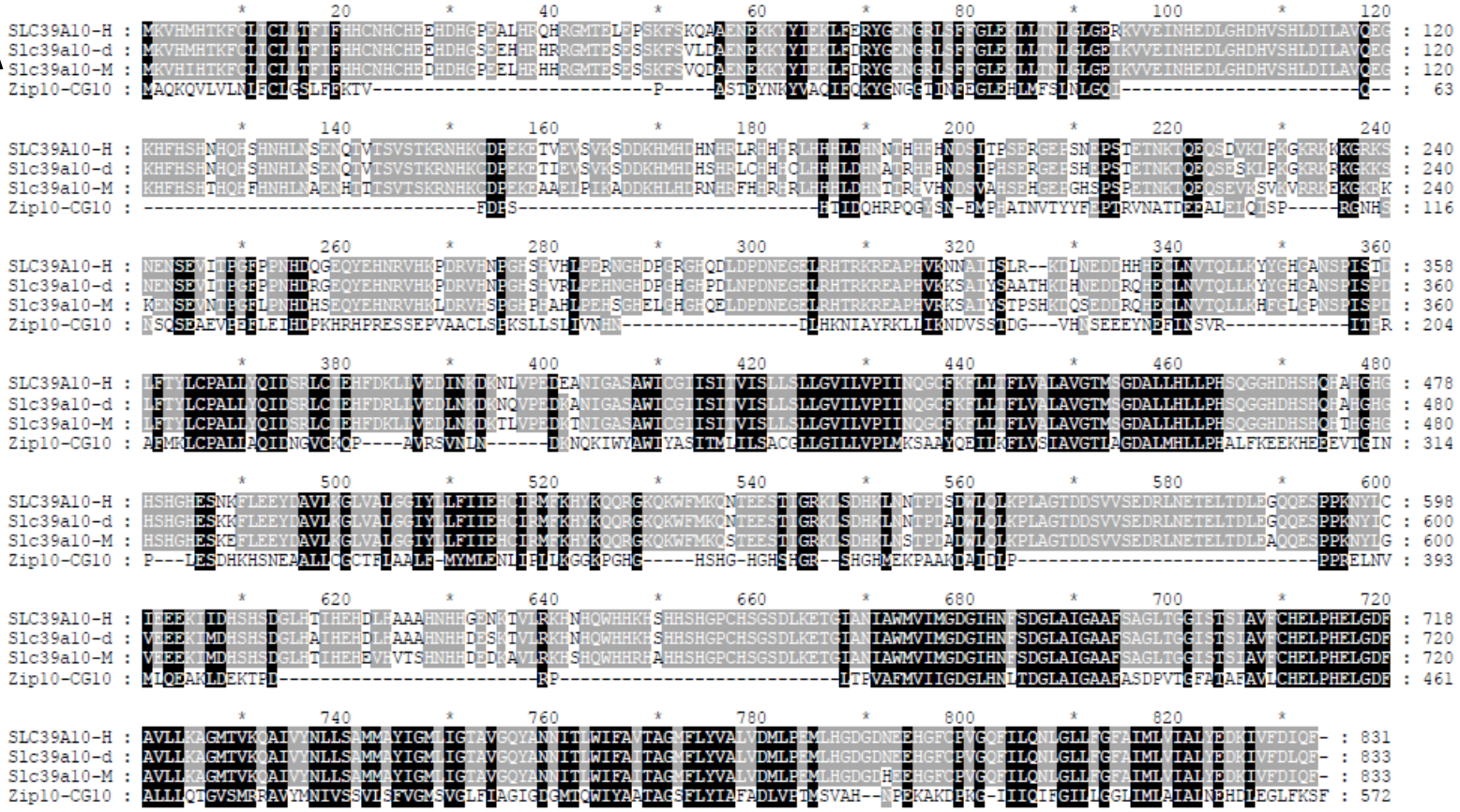

B

% identity

Divergence

	1	2	3	4	5	
1		93.3	87.3	29.2	27.9	SLC39A10-human
2	6.9		88.8	30.1	26.4	Slc39a10-dog
3	13.9	12.1		29.9	27.7	Slc39a10-mouse
4	159.5	155.2	155.9		27.6	Zip10-CG10006-Dros
5	151.6	156.1	155.8	168.5		foiA-cg6817

C

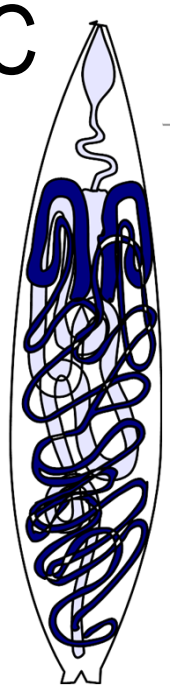

FlyAtlas Organ/Tissue Expression, larval vs. adult

Larval Expression Level	Tissue	Adult Expression Level
NA	Head	26.6
NA	Eye	22.525
NA	Brain	44.8
20.075	Central Nervous System	NA
NA	Thoracic-Abdominal Ganglion	49.8
NA	Crop	1.6
24.2	Midgut	22.8
12.5	Hindgut	35.8
3219.7	Malpighian Tubules	902.9
5.9	Fat Body	4.8
26.6	Salivary Gland	75.9
NA	Heart	1.95
33.4	Trachea	NA
NA	VirginFemale Spermatheca	2.8
NA	InseminatedFemale Spermatheca	4.1
NA	Ovary	0.5
NA	Testis	20.1
NA	Male Accessory Gland	3.4
37.525	Carcass	4.6

0-10 10-100 100-1000 1000-10000

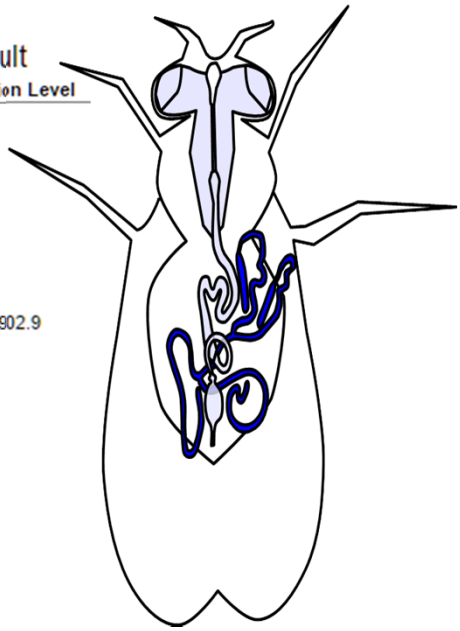

Figure 1

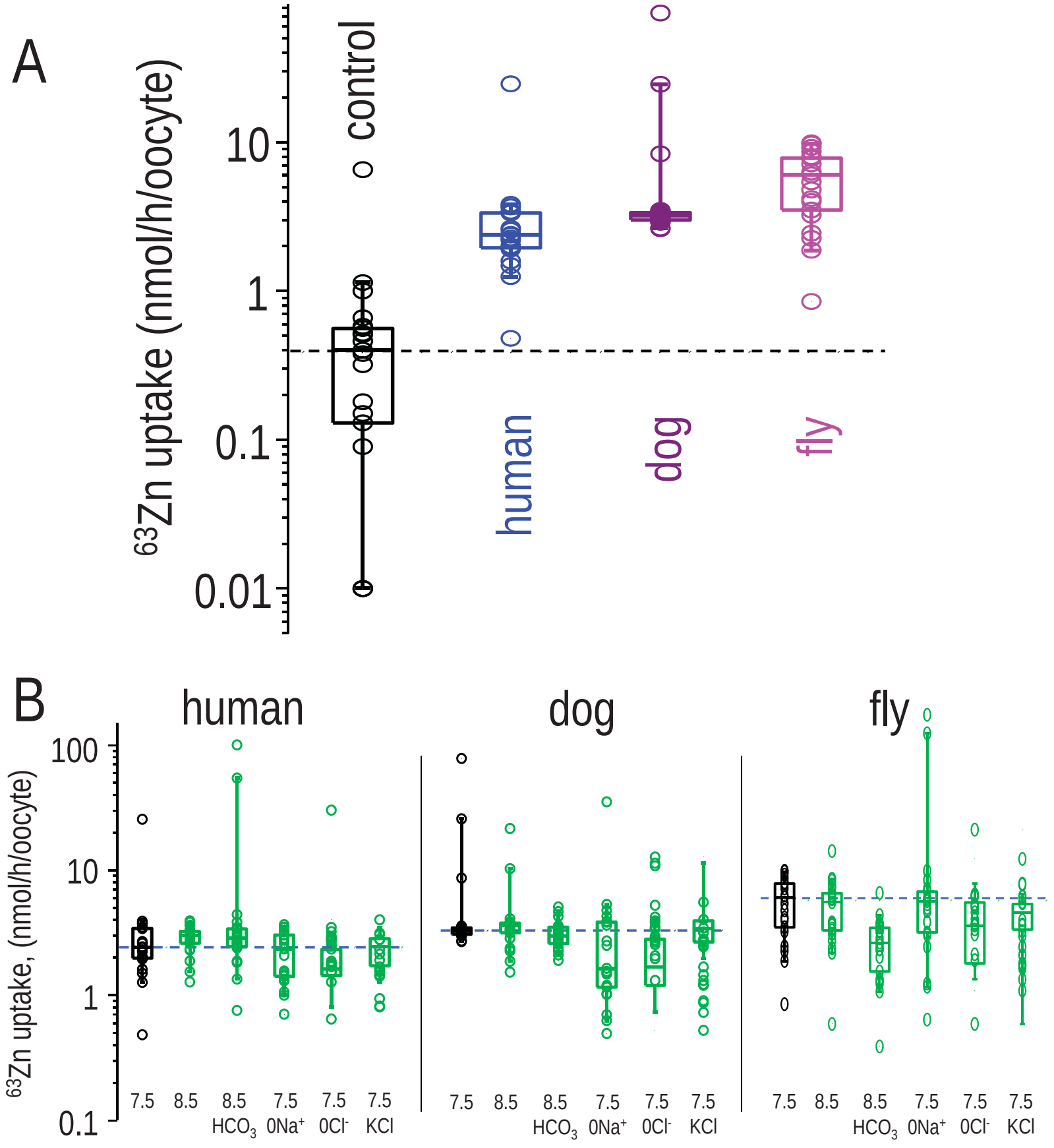
A
control
human
dog
fly
^{63}Zn uptake (nmol/h/oocyte)
10
1
0.1
0.01
B
human
dog
fly
^{63}Zn uptake, (nmol/h/oocyte)
100
10
1
0.1
7.5
8.5
8.5 HCO$_3$
7.5 0Na$^+$
7.5 0Cl$^-$
7.5 KCl

Figure 2

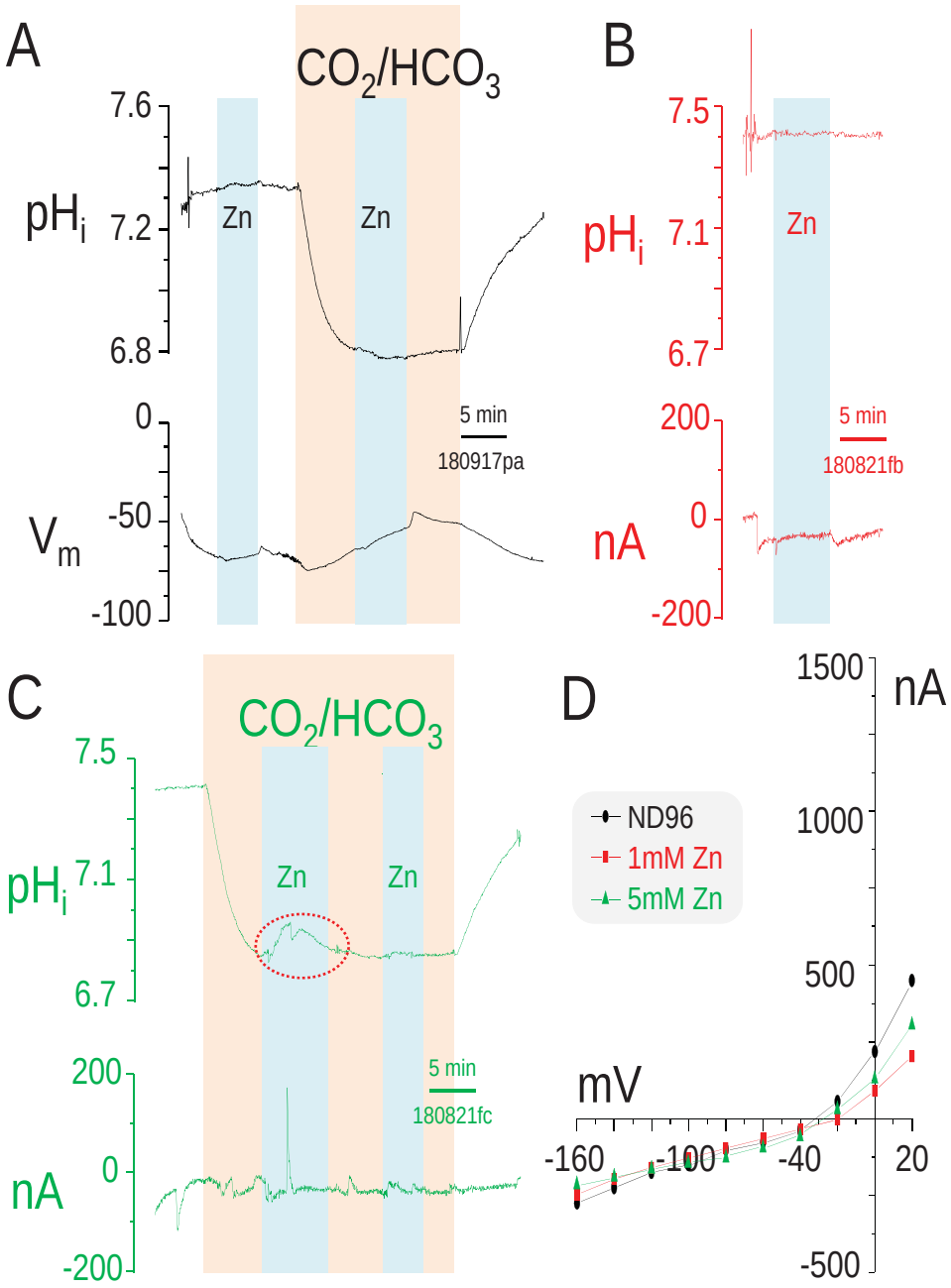
A
CO_2/HCO_3
7.6
pH_i
7.2
6.8
Zn
Zn
0
-50
V_m
-100
5 min
180917pa
B
7.5
pH_i
7.1
6.7
Zn
200
0
nA
-200
5 min
180821fb
C
CO_2/HCO_3
7.5
pH_i
7.1
6.7
Zn
Zn
200
0
nA
-200
5 min
180821fc
D
1500
nA
1000
ND96
1mM Zn
5mM Zn
500
mV
-160
-100
-40
20
-500

Figure 3

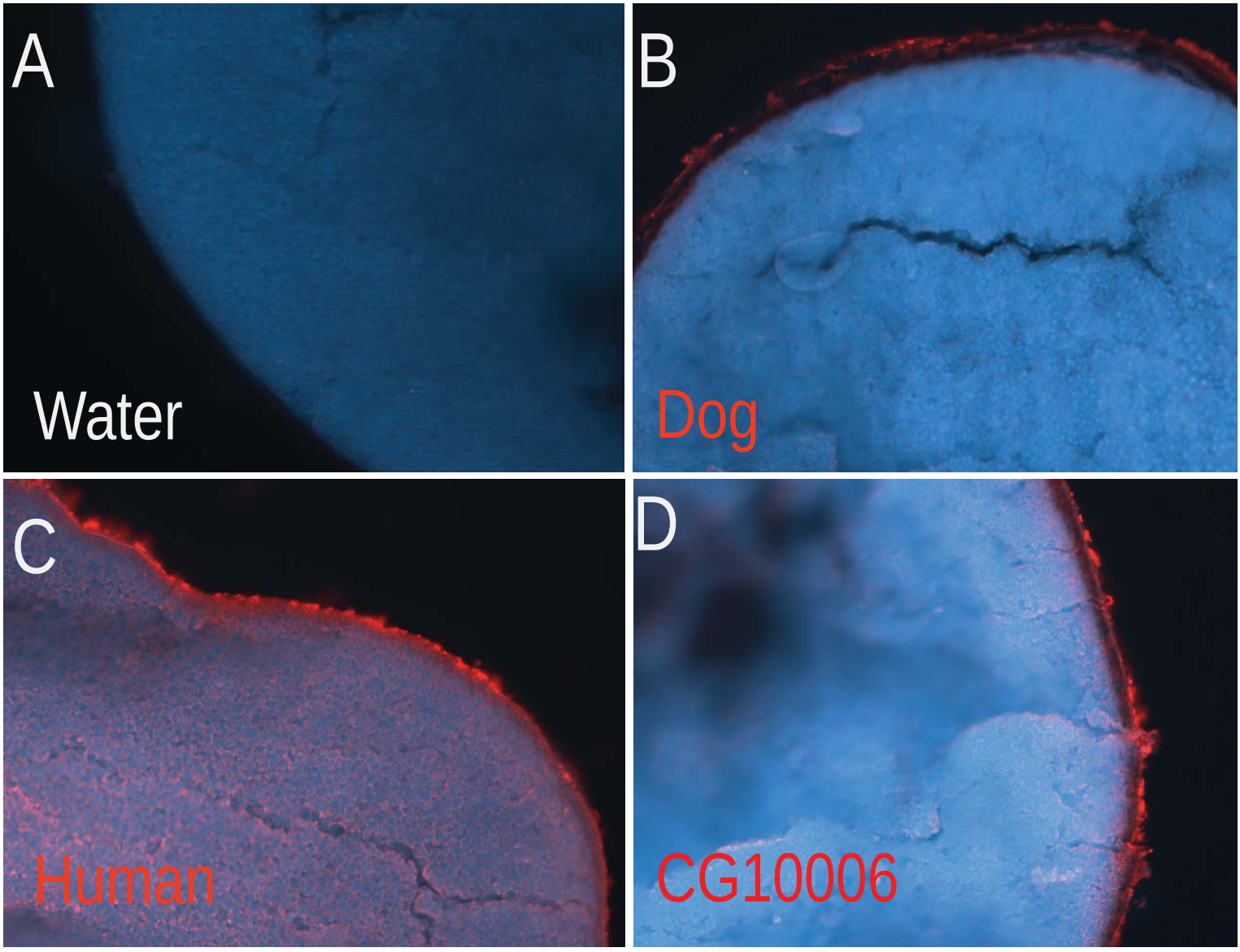

Figure 4

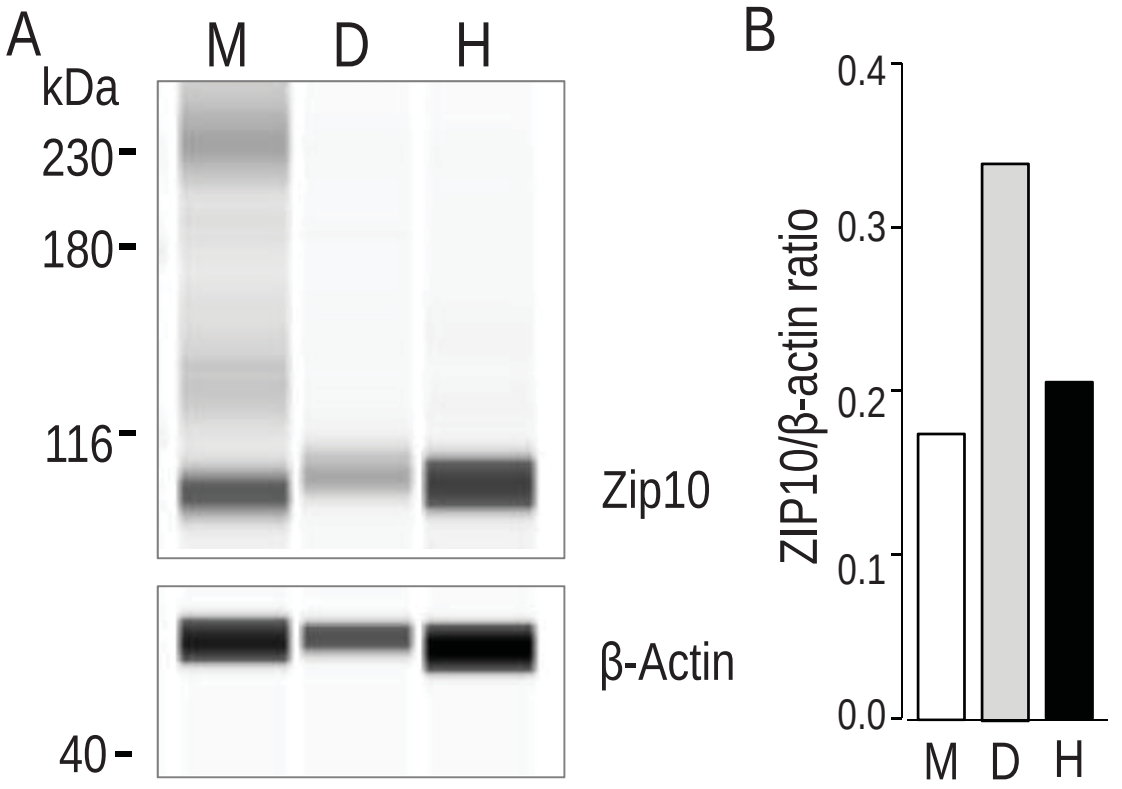
A
M
D
H
kDa
230
180
116
40
Zip10
β-Actin
B
ZIP10/β-actin ratio
0.4
0.3
0.2
0.1
0.0
M
D
H

Figure 5

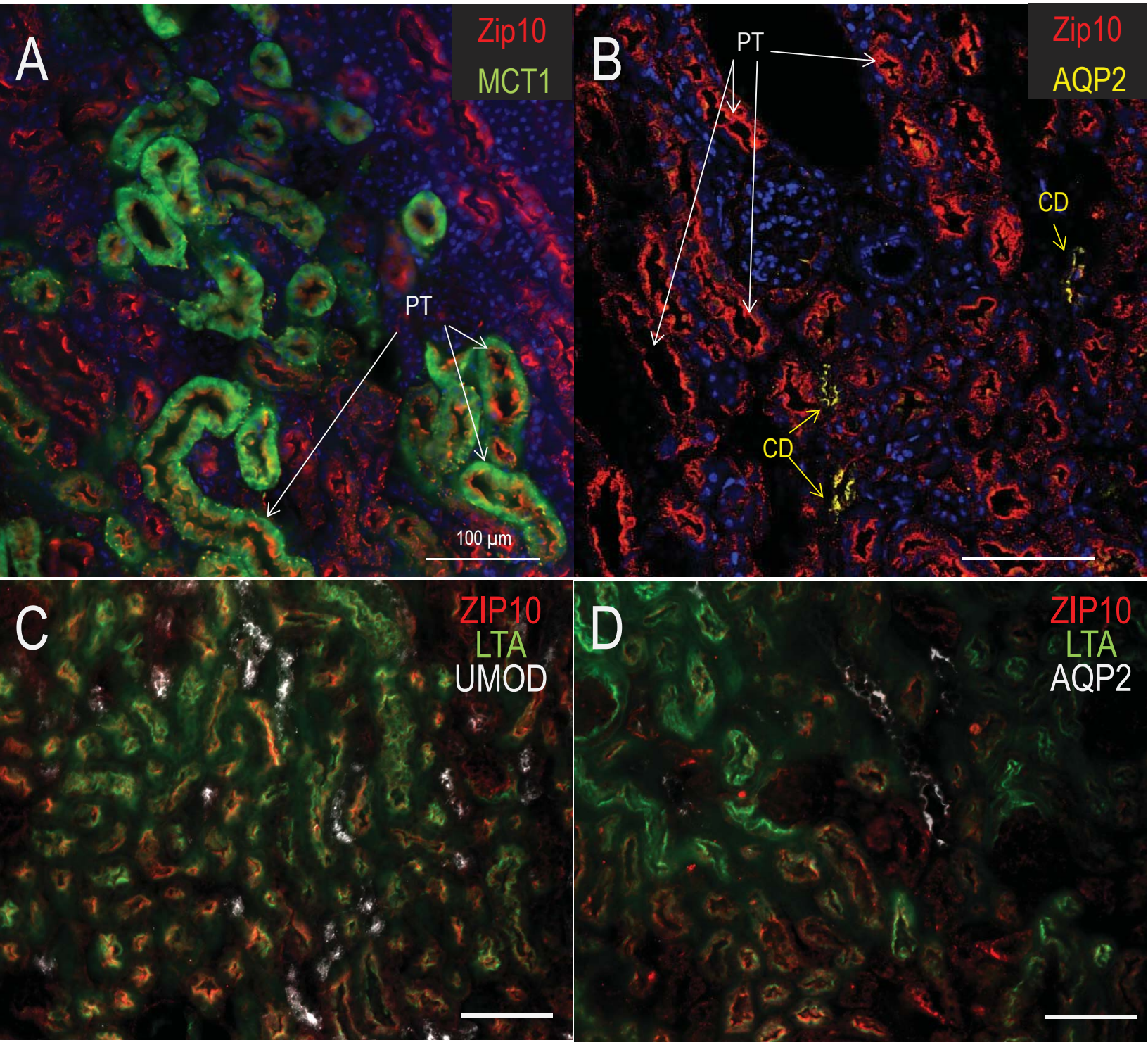
A
Zip10
MCT1
PT
100 µm
B
PT
Zip10
AQP2
CD
CD
C
ZIP10
LTA
UMOD
D
ZIP10
LTA
AQP2

Figure 6

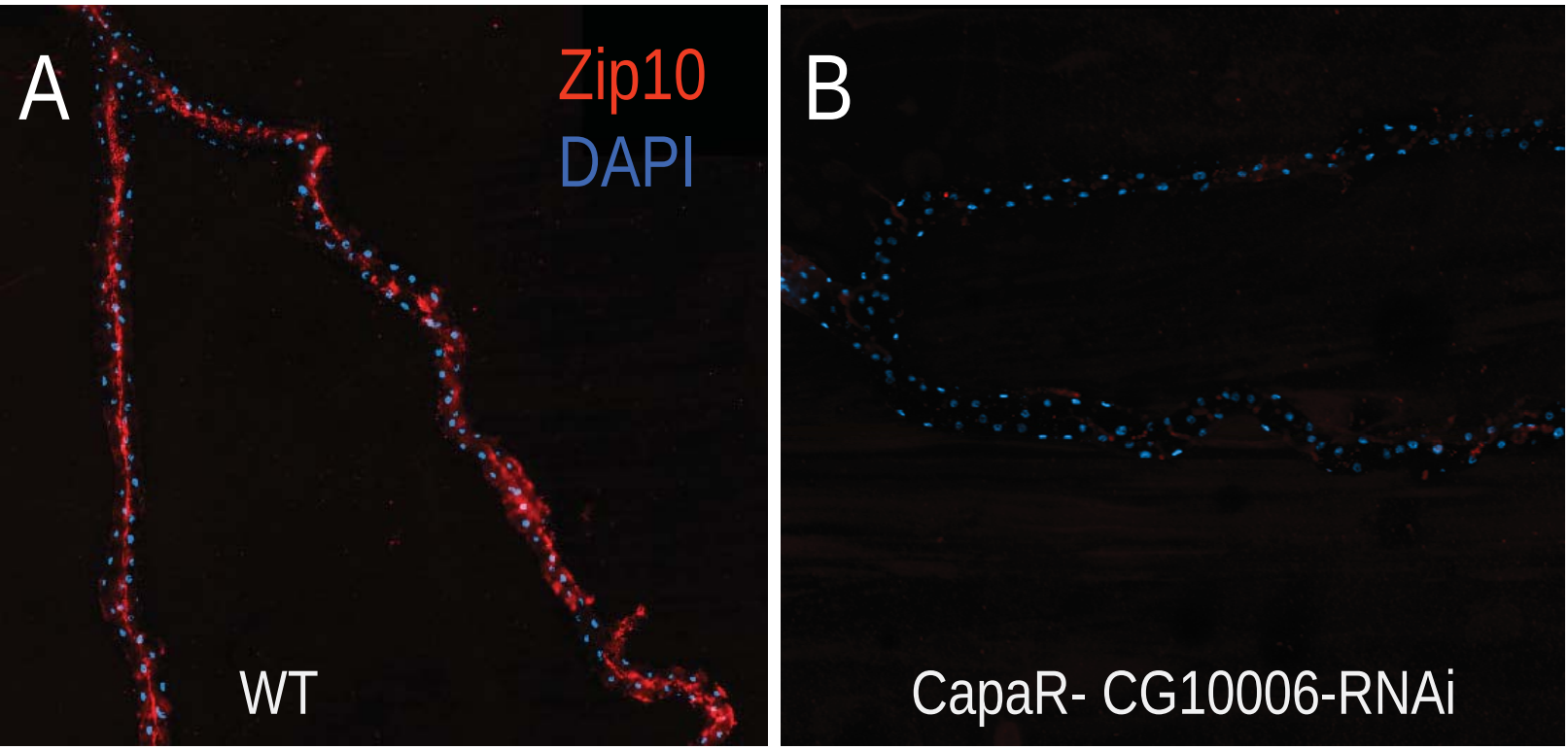

Figure 7

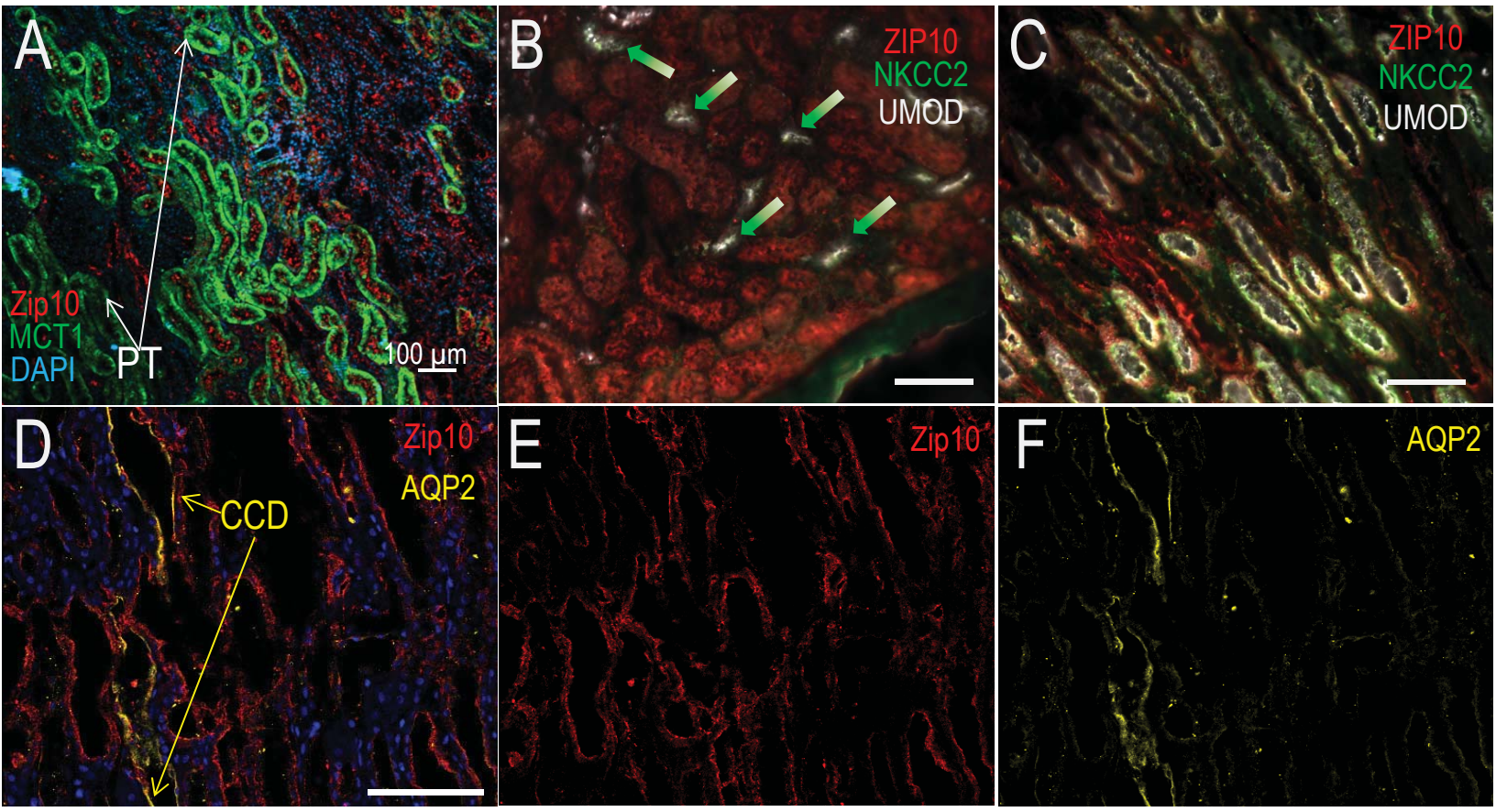
A
Zip10
MCT1
DAPI
PT
100 µm
B
ZIP10
NKCC2
UMOD
C
ZIP10
NKCC2
UMOD
D
Zip10
AQP2
CCD
E
Zip10
F
AQP2

Figure 8

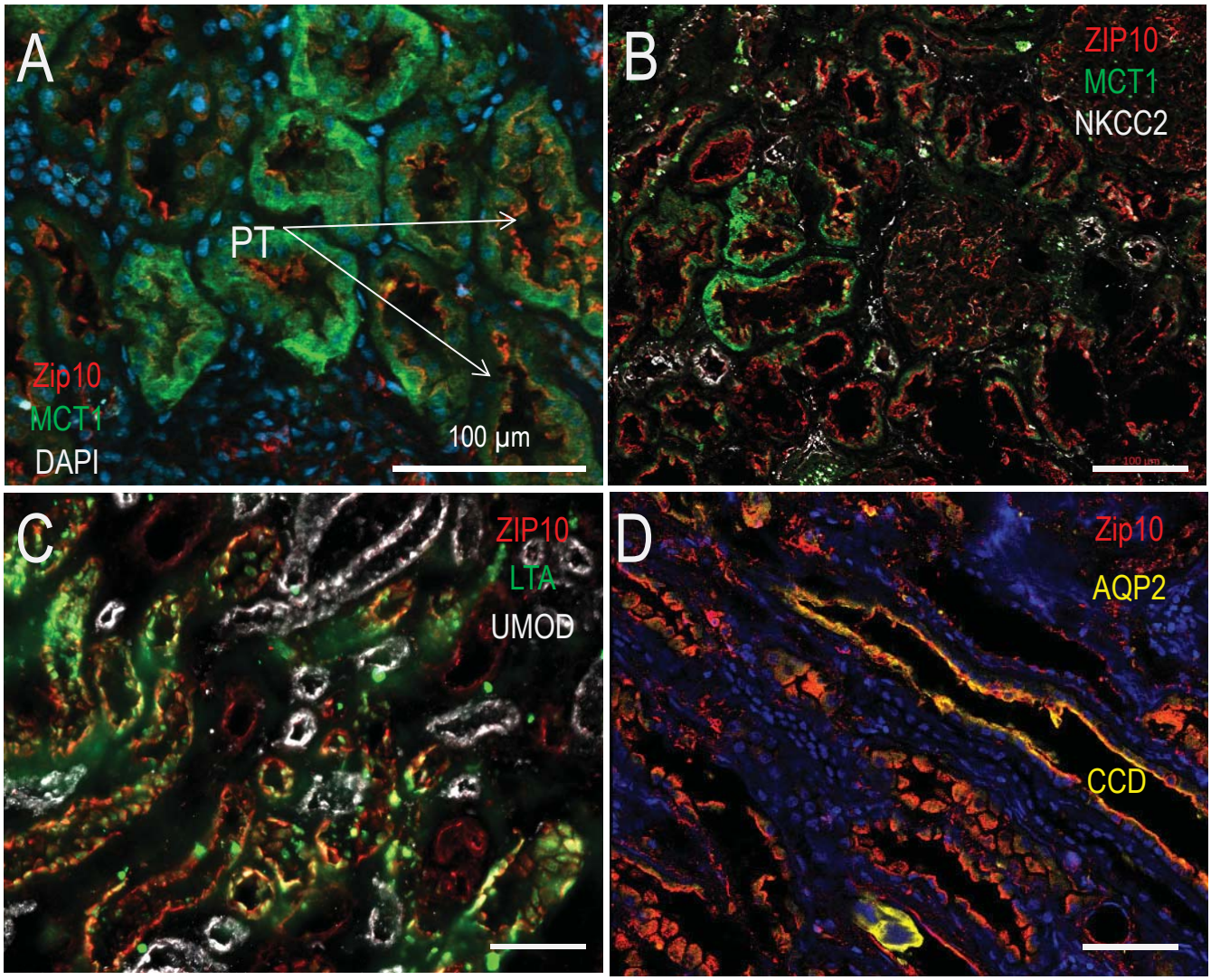
A
PT
Zip10
MCT1
DAPI
100 µm
B
ZIP10
MCT1
NKCC2
C
ZIP10
LTA
UMOD
D
Zip10
AQP2
CCD

Figure 9

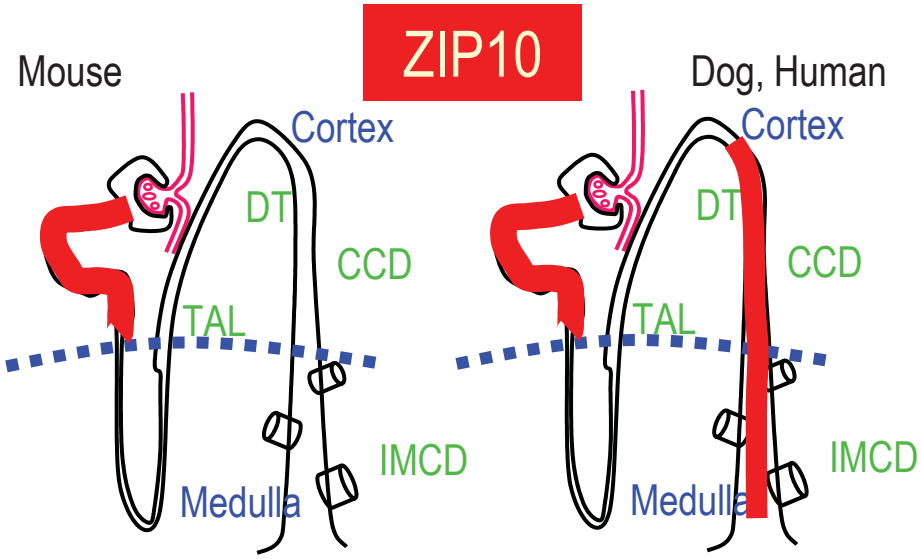
ZIP10
Mouse
Dog, Human
Cortex
DT
CCD
TAL
IMCD
Medulla
Cortex
DT
CCD
TAL
IMCD
Medulla

Figure 10